SLAC-PUB-2810
LBL-13360
September 1981
(T/E)

Baryon Production at PEP*

G. Goldhaber
Lawrence Berkeley Laboratory
and Department of Physics
University of California, Berkeley, California 94720

and

J. M. Weiss
Stanford Linear Accelerator Center
Stanford University, Stanford, California 94305

SLAC-LBL-Harvard Mark II Collaboration[1]

ABSTRACT

Measurements of inclusive $\Lambda+\bar{\Lambda}$ production for $1.0 < p < 10.0$ GeV/c and $p+\bar{p}$ production for $0.4 < p < 2.0$ GeV/c show significant baryon production in e^+e^- annihilation at $E_{c.m.} = 29$ GeV. $\Lambda+\bar{\Lambda}$ production represents 0.2 Λ's or $\bar{\Lambda}$'s per PEP event while the observed $p+\bar{p}$ production implies all baryon-antibaryon pair production is occurring at least as often as 0.6 per event, depending on the yet to be measured $p+\bar{p}$ production at high momentum. Comparisons are made with the first theoretical attempts to account for baryon production at these energies.

INTRODUCTION

We present measurements of inclusive Λ and proton production obtained with the Mark II detector running at PEP. A total of 5500 hadronic events have been observed from 15153 nb^{-1} integrated luminosity recorded at $E_{c.m.} = 29$ GeV between February and June, 1981. Some other Mark II results from this initial run are included in the talk of P. Söding which appears elsewhere in these proceedings.[2]

* Work supported by the Department of Energy, contracts DE-AC03-76SF00515 and W-7405-ENG-48.

(Presented at the Annual Meeting of the Division of Particles and Fields of the APS, Santa Cruz, California, September 8-11, 1981.)

SLAC-PUB--2810

DE82 005662

Λ AND $\bar{\Lambda}$ PRODUCTION

Λ and $\bar{\Lambda}$ hyperons are identified by their $p\pi^-$ and $\bar{p}\pi^+$ decay modes. Figure 1 shows the combined mass distribution with $1.0 < p_{\Lambda} < 10$ GeV/c. An rms resolution of 3.5 MeV with a total number of 95 Λ's and 70 $\bar{\Lambda}$'s is observed. Here time-of-flight information is used for protons up to 1.6 GeV/c. For higher momenta all tracks are tried as protons. In addition, in the vee reconstruction it is required that (i) the angle between the vee momentum and the line joining the secondary vertex with the origin be less than 8° and that (ii) the distance between the origin and the secondary vertex be at least 1.0 cm.

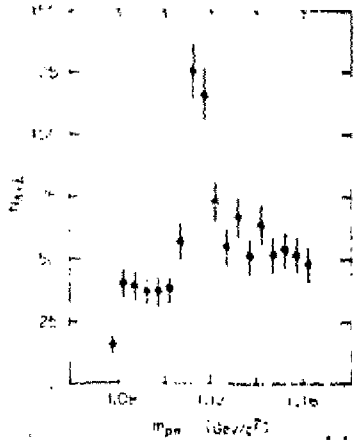

Fig. 1. Invariant mass distribution for Λ+$\bar{\Lambda}$ events.

The proper time distribution for the Λ and $\bar{\Lambda}$'s, after background subtraction, is shown in Figure 2. We observe a value $c\tau = 6.4 \pm 1.9$ cm which is consistent with the established value of $c\tau = 7.9$ cm (dashed line).

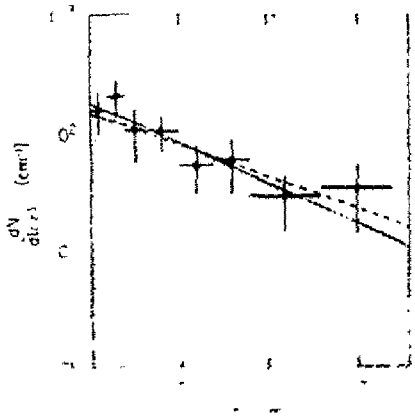

Fig. 2. Proper lifetime distribution of Λ+$\bar{\Lambda}$ events.

A similar analysis, with the additional requirement that the distance of closest approach of each pion with the intersection point be greater than 3.5 mm, yields the K^0_S mass distribution plotted in Figure 3 and the K^0_S proper time

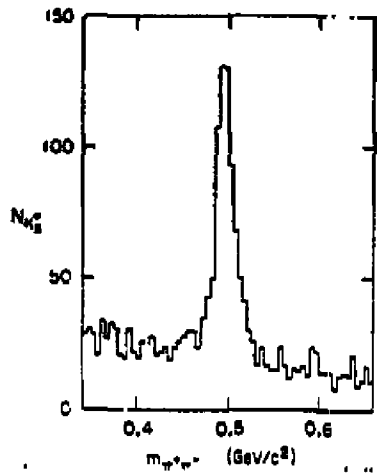

Fig. 3. Invariant mass distribution for K^0_S.

distribution shown in Figure 4. Again the measured value $c\tau$ = 2.75 ± 0.27 cm is in good agreement with the nominal value $c\tau$ = 2.68 cm.

Inclusive cross-sections for Λ and K^0 production are determined using efficiencies obtained with a version of the OCD Monte Carlo of Ali et al.[3] which has been modified to include baryon production. Radiative corrections have not yet been applied. Cross-sections $d\sigma/dp$ are plotted in Figure 5 along with recent results from the TASSO[4] and JADE[5] collaborations which are presented elsewhere in these proceedings by S. Wu.[6] The TASSO measurements are over the same momentum range of 1-10 GeV/c and are in good agreement with our results.

$p+\bar{p}$ PRODUCTION

Protons and antiprotons are identified by time-of-flight techniques. Figure 6 presents a scatterplot of m^2, determined from the TOF and the momentum p, versus p for tracks in hadronic events. Each scintillator used here is required to have been traversed by only one reconstructed track. A time-of-flight weight for each track is then formed under the proton hypothesis

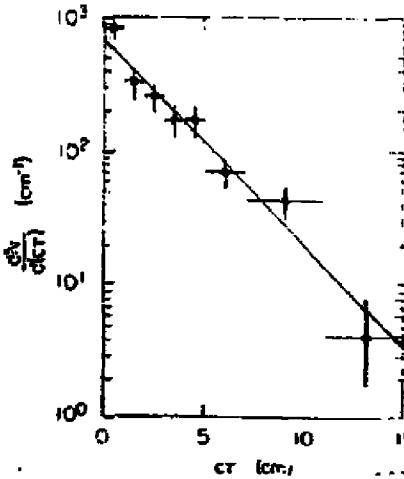

Fig. 4. K^0_S proper lifetime distribution.

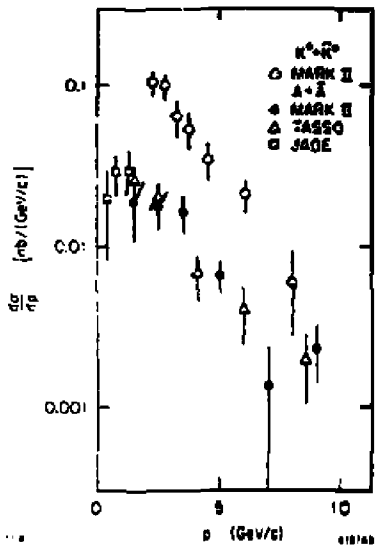

Fig. 5. Production cross-sections for $\Lambda+\bar{\Lambda}$ and $K^0+\bar{K}^0$.

$$w_p = e^{-(t-t_p)^2/2\sigma^2}$$

where t is the measured time and t_p is the expected time-of-flight for a proton. This is then renormalized by the sum of similar weights for pion, kaon and proton hypotheses, as described earlier.[7] Present resolution is σ = 360 psec for hadron tracks which is degraded from the SPEAR value of 300 psec due to increased scintillator attenuation length observed to have occurred since our running at SPEAR. Particles are identified as protons when the renormalized weight $w_p > 0.5$ for $0.4 < p < 1.4$ GeV/c or $w_p > 0.7$ for $1.4 < p < 2.0$ GeV/c. The background of misidentified hadrons, evident at high momentum in Figure 6, is subtracted using a careful simulation of the TOF response to calculate the number of non-proton tracks in the Monte Carlo which pass the proton weight cuts at each momentum.

Although the background subtraction is important (25-40%) for momenta $1.4 < p < 2.0$ GeV/c, Figure 7 shows that a clear $p+\bar{p}$ signal is

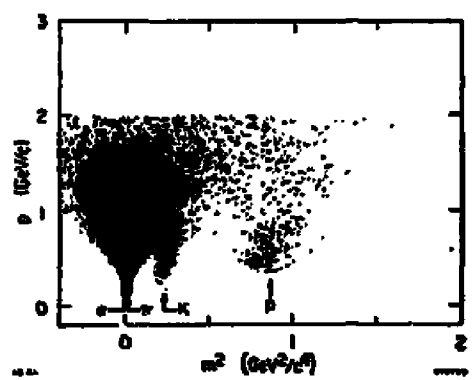

Fig. 6. m^2 vs p from the TOF measurement.

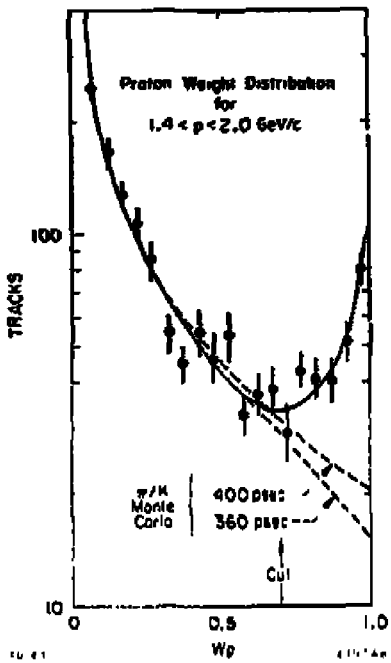

Fig. 7. Distribution of proton time-of-flight weights for $p > 1.4$ GeV/c.

visible in the proton weight distribution. The dashed curves in Figure 7 show the Monte Carlo expectations for non-proton tracks with different time-of-flight resolutions. The cross-section errors presented below include estimates of the uncertainty in the subtraction from variation of the number of kaons and from non-Gaussian resolution tails. Both these effects are strongly constrained by the data.

The $p+\bar{p}$ cross-sections, $d\sigma/dp$, which result are plotted in Figure 8 along with the recent results of the TASSO[8] and JADE[4] collaborations at PETRA. Agreement among the 3 experiments is reasonably good, although our cross-sections may be somewhat higher than the single TASSO point at the higher end of the momentum range. Radiative corrections have not been applied to our data.

Our data, however, show a significantly higher cross-section at momenta near 2 GeV/c than is predicted by the Lund group's QCD Monte Carlo[9] (solid line in Figure 8). As a first effort to describe baryon production, this model neglects Λ_c production and leading baryons and has had its parameters fixed using the SPEAR data near $E_{c.m.} = 5$ GeV. Our data indicate that further adjustment of the parameters, or some additional dynamics in the model, is required. Qualitative agreement, however, of both the p and Λ cross-sections with the predictions of the model can be obtained, as shown in Figure 9, if we increase the normalization by ~1.25.

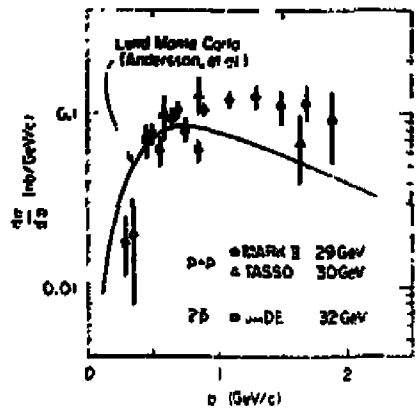

Fig. 8. Production cross-sections for $p+\bar{p}$.

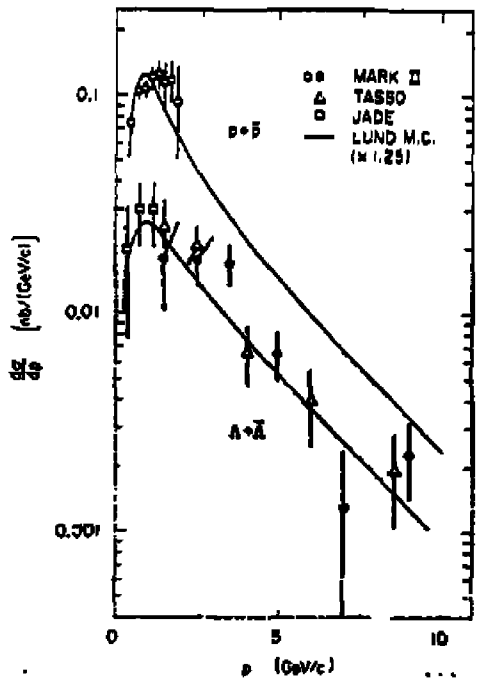

Fig. 9. Comparison of $d\sigma/dp$ with the Lund Monte Carlo. The curves come from S. Wu, Talk given at the SLAC Summer Institute Topical Conference, July-August 1981, but have been scaled by 1.25.

$R(\Lambda+\bar{\Lambda})$ AND $R(p+\bar{p})$ MEASUREMENTS

The values of R observed in their respective momentum ranges are:

$$R(\Lambda+\bar{\Lambda}) = 0.72 \pm 0.18 \qquad 1 < p < 10 \text{ GeV/c}$$

$$R(p+\bar{p}) = 1.66 \pm 0.25 \qquad 0.4 < p < 2.0 \text{ GeV/c}$$

and these are plotted in Figures 10(a) and 10(b) along with previous measurements.

One can use the exponential behavior exhibited by the cross-section, $(E/4\pi p^2)\, d\sigma/dp$ within these momentum ranges[10] to extrapolate beyond them. For the $\Lambda + \bar{\Lambda}$'s, an exponential e^{-bE} with $b = 0.9 \pm 0.1$ GeV^{-1} is observed and leads to a relatively small correction which gives $R(\Lambda+\bar{\Lambda}) = 0.80 \pm 0.24$ extrapolated to all momenta. Here the error includes the estimated systematic error of the extrapolation. In the more limited range of proton momenta, a slope $b = 1.6 \pm 0.2$ GeV^{-1} behavior well describes the invariant cross-section and leads to an extrapolated value of $R(p+\bar{p}) = 2.48 \pm 0.62$ which is plotted in Figure 10(c) along with the extrapolated Λ results. The proton extrapolation, however, has substantial uncertainty due to the large unobserved range of momentum. A flattening of the proton invariant cross-section at higher momentum similar to

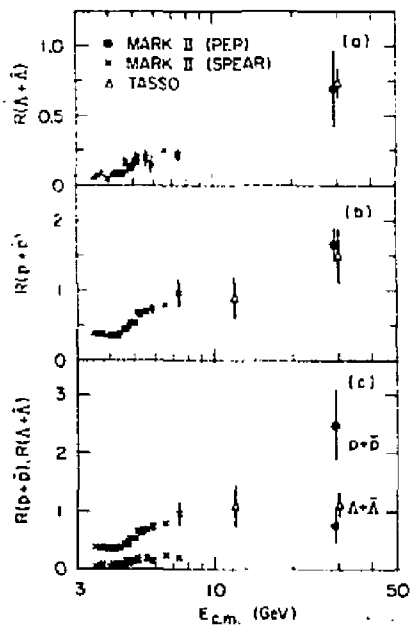

Fig. 10. R-values vs energy for (a) $R(\Lambda+\bar{\Lambda})$ and (b) $R(p+\bar{p})$ in their observed momentum ranges and (c) both $R(\Lambda+\bar{\Lambda})$ and $R(p+\bar{p})$ after extrapolation to all momenta.

the observed Λ's would increase $R(p+\bar{p})$ by about 40%. Thus, in a sense, the extrapolated $R(p+\bar{p})$ value plotted in Figure 10(c) represents a lower limit which corresponds to 0.6 baryon-antibaryon pairs per event at PEP.

SOME INTERESTING EVENTS

Two interesting events observed in this analysis are shown in Figures 11 and 12. Figure 11 shows a two-jet event which contains $2K_S^0$'s and nothing else detected. The $K_S^0K_S^0$ mass is 3.4 GeV/c^2. Figure 12 shows a two-jet event with a Λ and $\bar{\Lambda}$, as well as several γ's, in one of the jets. The $\Lambda\bar{\Lambda}$ mass is 2.6 GeV/c^2.

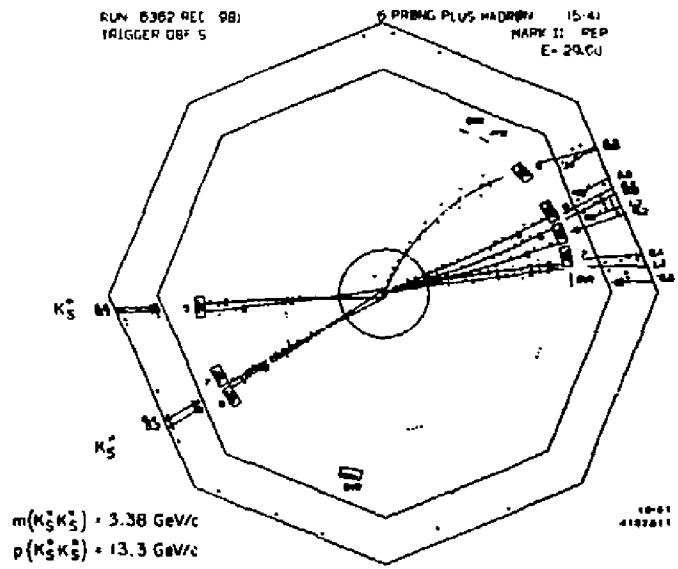

Fig. 11. Event #1.

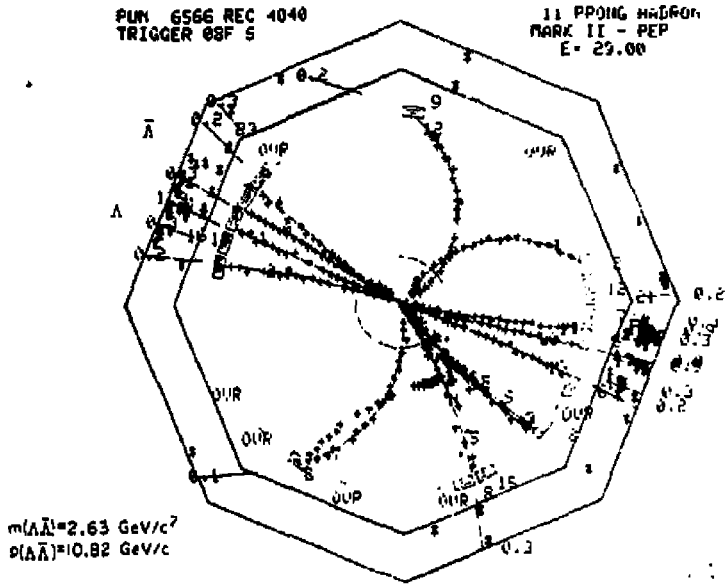

Fig. 12. Event #2.

CONCLUSIONS

Events containing both p and $\bar{p}$ are obtained and these are presently under study (along with a number with pp or $\bar{p}\bar{p}$). In addition, substantial Monte Carlo work is beginning with both the Lund model and with our own modifications of the popular Ali QCD jet model.

These first results show baryons are clearly playing a fairly substantial role in e^+e^- annihilation at PEP and PETRA. Hopefully, future work will lead us to understand in some detail the mechanism(s) responsible for their production and, perhaps, thereby to a deeper understanding of the workings of QCD.

REFERENCES

1. G. S. Abrams, D. Amidei, A. Backer, C. A. Blocker, A. Blondel, A. M. Boyarski, M. Breidenbach, D. L. Burke, W. Chinowsky, M. W. Coles, G. von Dardel, W. E. Dieterle, J. E. Dillon, J. Dorenbosch, J. M. Dorfan, M. W. Eaton, G. J. Feldman, M. E. B. Franklin, G. Gidal, L. Gladney, G. Goldhaber, L. Golding, G. Hanson, R. J. Hollebeek, W. R. Innes, J. A. Jaros, A. D. Johnson, J. A. Kadyk, A. J. Lankford, R. R. Larsen, B. LeClaire, M. Levi, N. Lockyer, B. Lohr, V. Lüth, C. Matteuzzi, M. E. Nelson, J. F. Patrick, M. L. Perl, B. Richter, A. Roussarie, D. L. Scharre, H. Schellman, D. Schlatter, R. F. Schwitters, J. L. Siegrist, J. Strait, G. H. Trilling, R. A. Vidal, I. Videau, Y. Wang, J. M. Weiss, M. Werlen, C. Zaiser, and G. Zhao, Stanford Linear Accelerator Center, Stanford University, Stanford, California 94305, Lawrence Berkeley Laboratory and Department of Physics, University of California, Berkeley, California 94720, Department of Physics, Harvard University, Cambridge, Massachusetts 02138.
2. P. Söding, Proceedings of the APS DPF Conference, U.C. Santa Cruz, September 8-11, 1981.
3. A. Ali et al., Phys. Lett. 93B, 155 (1980).
4. R. Brandelik et al., DESY 81/039 (July 1981). (Submitted to Phys. Lett.)
5. W. Bartel et al., Phys. Lett. 104B, 325 (1981).
6. S. Wu, Proceedings of the APS DPS Conference, U.C. Santa Cruz, September 8-11, 1981.
7. G. S. Abrams et al., Phys. Rev. Lett. 44, 10 (1980); J. M. Weiss et al., Phys. Lett. 101B, 439 (1981).
8. R. Brandelik et al., Phys. Lett. 94B, 444 (1981).
9. B. Andersson et al., Lund LU TP 81-3 (April 1981). The curve in Fig. 8 is from a private communication with these authors and is for $E_{c.m.}$ = 29 GeV without radiative corrections.
10. This corresponds precisely to the relativistic invariant cross-section, $E\, d^3\sigma/dp^3$, for an isotopic angular distribution and to good approximation for the (extreme) $1 + \cos^2\theta$ inclusive angular distribution.